Available online at www.sciencedirect.com

ScienceDirect

Procedia CIRP 81 (2019) 771–774

www.elsevier.com/locate/procedia

52nd CIRP Conference on Manufacturing Systems

A visual inspection system for KTL coatings

Drago Bračun[a*] and Igor Lekše[b]

[a]University of Ljubljana, Faculty of Mechanical Engineering, Aškerčeva cesta 6, SI-1000 Ljubljana
[b]TPV d.o.o., Kandijska cesta 60, SI-8000 Novo mesto

* Corresponding author. Tel.: +386-1-4771 747; fax: + 386-1-2518 567. E-mail address: drago.bracun@fs.uni-lj.si

Abstract

Many metal components in automotive industry are surface-protected using the electrophoretic cathode metal coating (KTL). As surface defects can occur in this process, the components need to be 100% inspected, especially if the manufacturers are committed to delivering zero-defect products. Due to complicated 3D curved shapes and black shiny colour of the coating, inspection is typically carried out manually. To avoid labour-intensive manual inspection in serial production, an automated visual inspection system is developed. The paper presents the implementation of a control device for mass inspection of the products, typical KLT coating defects, and the visual inspection method for the detection of coating defects. A difference image acquisition method is implemented in order to reveal the defects on the black shiny colored parts. An image processing algorithm for the recognition of light patterns and a clustering approach for the recognition of defects are presented.

Keywords: KTL; surface defect; inspection; imaging system; pattern recognition; cluster

1. Introduction

Electrophoretic cathode metal coating (KTL or E-coat) [1] is an important technological process for painting and protecting the parts from environmental impacts. The quality of coating is achieved by managing the coating process and by inspecting parts after coating. There are a number of different coating defects, including: craters (bowl-shaped depressions), roughness (patches on a cured film that exhibits an alternately non-uniform and smooth appearance), redissolution (part of the coat film washes off or dissolves), dirt (three sources: process, environmental and oven), streaking (due to pretreatment, rinsing and racking), pinholing (a pattern of relatively small, random volcano-like holes), air entrapment, gloss variations, color variations, thin coating, corrosion and orange peel. Example of defects are shown in Fig. 1. Coating defects on products should be identified immediately after the coating process. For that purpose, coated parts are visually inspected. Because of complicated shapes and black shiny color of the coating, inspection is typically carried out manually. Regardless of the staff experience, manual inspection is subjective and time-consuming in large-series production.

The literature review shows several specific solutions for surface defect detection. The system described in [2] acquires multiple images under different lighting conditions, and then these images are processed separately and merged into one. The features extracted from this fused image and the former processing steps establish the feature space for a supervised learning classifier based on artificial neural networks. The system presented in [3] detects defects catalogued as dings and dents on car body surfaces. It sweeps the object with the light patterns, and uses image fusion based on optical flow to obtain a resulting fused image which holds the information of all variations suffered by the projected patterns during the sweeping process, indicating the presence of anomalies. A deflectometry method [4] features a high resolution camera and a dedicated illumination system based on displaying fringe patterns in a monitor, allowing the detection of irregularities in surfaces. An overview of three different image acquisition

2212-8271
10.1016/j.procir.2019.03.192

approaches for automatic visual inspection of metallic surfaces is presented in [5]. The first method is gray-level intensity imaging with bright and dark field lighting techniques. Subsequently, two range imaging techniques are introduced which may succeed in contrast to intensity imaging if the reflection property across the intact surface changes. However, range imaging for surface inspection is restricted to surface defects with three-dimensional characteristics, e.g. cavities.

A surface defect detection system for mobile phone screen glass [6] corrects the image misalignment and then the combination of subtraction and projection is used to identify defects. To segment the defects, an improved fuzzy c-means cluster algorithm is developed.

The vision system for on-line surface inspection in an aluminum casting process [7] implements similarity-based algorithms as well as texture algorithms for defect detection in a high-textured surface where, for most defects, segmentation cannot be achieved solely by means of threshold techniques. The system was applied to continuous cast aluminum inspection, where up to fifteen different kinds of defects must be detected and classified.

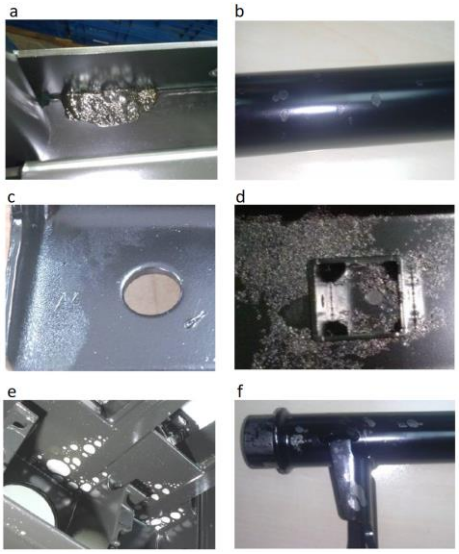

Fig. 1. Examples of coating defects: (a) coagulated paint; (b) air entrapment; (c) roughness; (d) corrosion; (e) redissolution; (f) dirt.

2. Automated visual inspection system

The automated visual inspection system presented in Fig. 2 is integrated into the part transportation system from the KTL process to the automated warehouse. The part transportation system is carried out with AGV's and industrial robots, as is demonstrated in Fig. 3. The inspection is carried out employing 16 cameras and carefully designed illumination for each camera. The inspection device has four nests, of which the first and the last are used for robotic part handling, and the middle two are intended for visual inspection. Part transportation between the nests is carried out with two servo-drive based part transportation systems. The control of the device is carried out with the PLC and i7 based industrial PC for image processing. The challenges which were encountered and are presented in the continuation of this paper are detection of defects on complicated 3D curved shapes with black shiny coating (see Fig. 4) and the distinction between critical defects and visual flaws.

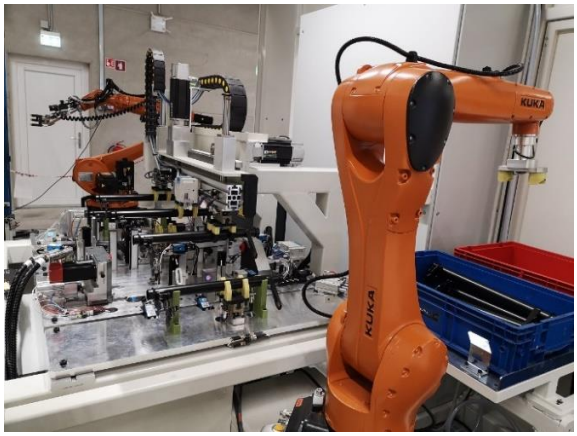

Fig. 2. Automated visual inspection system [8].

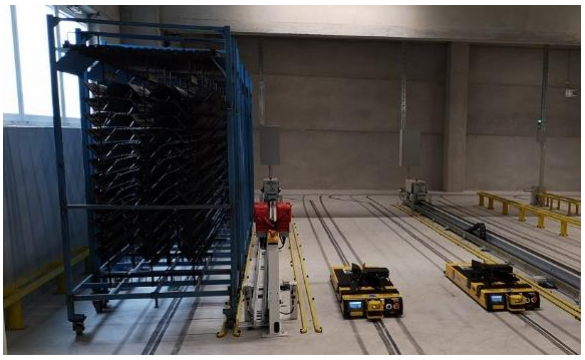

Fig. 3. Part transportation system with AGV-s.

3. Image processing

Coating defects are usually visible as blobs of different image brightness, as is demonstrated in Fig. 4. They are typically brighter than their surroundings, varying in size from a few pixels to larger parts of the image. They can also take the form of a cluster of small blobs. In the image processing stage, these light blobs are initially extracted from the image and then classified either as actual defects or as visual flaws. Their extraction is carried out first by employing threshold values to the image to obtain a mask in form of binary image, with pixel values 0 or 1. The value is 1 if the pixel brightness in the image of interest is brighter than the threshold value, and 0 if it is below. Blobs are identified as areas where the value of adjacent pixels is 1. After being identified, their area i.e the number of adjacent pixels with value 1, is calculated. The initial criterion for the defect identification is the area of the blob as well as other geometric properties, e.g. location and shape.

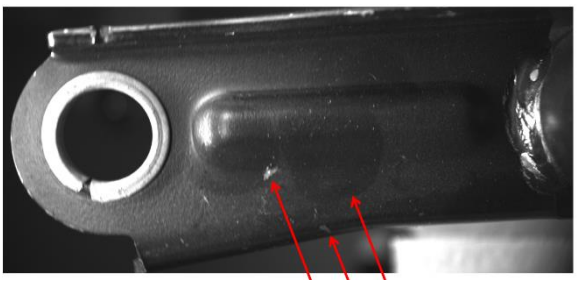

Fig. 4. Image ***A***. A detail of a typical KTL-coated part with 3D form and black shiny color. Arrows point to the coating damage, dust and fingerprint.

However, blob extraction is not so straightforward since the coated objects are curved in all directions. Feature recognition in imaging systems typically starts with the illumination of the object, which should be adjusted so as to reveal the features of interest, i.e. bright or dark field illumination. At curved objects, it is not possible to adjust the illumination to all object features, and from some parts of the object a bit of light reflection will occur directly in the camera while at others the light will reflect away. These reflections resemble the defects in image, which interferes with image processing.

One solution to the problem is to create a background image ***B*** (see Fig. 5) that is subtracted from the image of interest ***A*** (see Fig. 4). The background image represents the average of a large number of images under the same lighting conditions and the same image acquisition setup. These images are acquired by inspecting the same type of product in many products without defects (>20).

Fig. 5. The background image ***B***. It is the average of a large number of images (>20) under the same lighting conditions and the same image acquisition setup.

Fig. 6. The difference image ***D*** *is the image* ***A*** *with removed background* ***B***.

By subtracting the background image ***B*** from the image of interest ***A*** and calculating the absolute value of the differences, we eliminate brightness variations caused by the object form. If we assume that images ***A***, ***B*** and ***D*** are arrays of same size and data type, with number of rows U and columns V, where and indices i,j index pixel values from i = 0 to U, and j = 0 to V. The difference image is calculated pixel wise as $\boldsymbol{D}_{i,j}=\text{abs}(\boldsymbol{A}_{i,j} - \boldsymbol{B}_{i,j})$, where abs stands for absolute value (see Fig. 6). If there are visible defects in image ***A***, they are also present in difference image ***D***, which can be observed by comparing Fig. 4 and Fig. 6.

The weak point of this method is in the alignment of images. The object of interest must be at the same position on both images. This cannotbe perfectly achieved, because there are two main sources of misalignment or variability: the first is variability among parts, i.e. how repeatable their dimensions are, and the second is in positioning of products inside the inspection device. Both can be minimized to a certain extent, but never completely eliminated. To deal with them, a software alignment of images is carried out based on Euclidean motion, where the first image is rotated and shifted with respect to the second image. There are three parameters (T_x , T_y) for translation and angle φ for rotation. The estimation of all motion parameters can be time-consuming in case of many large images. A simplification based on the knowledge of the product clamping inside the inspection device can be carried out. It was found that variability is most significant in positioning the part inside the inspection device and that the main motion is rotation, while the translation can be neglected. In addition, since the point of rotation is known, it is only necessary to identify the value of rotation. The search algorithm is straightforward: (*i*) rotate the image ***A*** with respect to the image ***B*** in sequence of small steps, (*ii*) in each step calculate the difference image ***D*** and (*iii*) calculate the sum off all pixels on the image ***D***. The rotation angle with the minimum sum is the best alignment angle.

Variability in dimensions among parts still remains and is most noticeable in the image ***D*** at the edges of the product where there is no overlap between the parts due to difference in shape (see Fig. 6). These bright edges are removed employing an additional mask that specifies the region of interest. Further image processing continues as already described at the beginning of this chapter, by thresholding, blob search, calculation of blob properties and defect identification.

4. Defect identification

In many cases, defects do not take the form of big blobs but rather appear as concentrated groups of small blobs. Fig.7 shows such an example. The left white circle marks a group of large area blobs that are actually a surface defect, while the right circle marks the group of small blobs that show dust on the surface and are not a defect. Defect identification that searches for a big blob does not recognize any of these blobs as a defect. To solve this problem, the blobs are grouped into clusters, and for each cluster the parameter quantifying the likelihood of a defect is calculated.

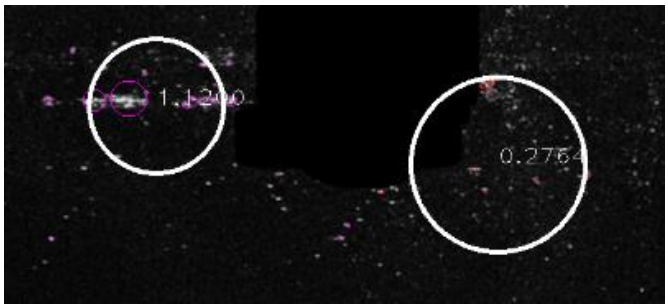

Fig. 7. Defects are visible as groups of small blobs.

For grouping the blobs, a *k-means* clustering algorithm is employed. The basic idea behind this clustering is to define clusters such that the total intra-cluster variation is minimized. The standard *k-means* clustering algorithm defines the total within-cluster variation as the sum of squared Euclidean distances (*total within-cluster sum of squares* **TSS**) between items (blob centers) and the corresponding cluster centroid.

Let us assume that we arrive at k clusters. For each cluster from k = 1 to K a total area of all blobs can be calculated as

$$A_k = \sum_{l=1}^{N} a_l, \tag{1}$$

where a_l is the blob area and N is the number of blobs in cluster k. Similarly, a cluster mean radius R_k is calculated as

$$R_k = \frac{\sum_{l=1}^{N}(r_l \cdot a_l)}{A_l}, \quad (2)$$

where r_l is the distance from the cluster centroid to the center of l-th blob. The parameter E which we use to quantify the likelihood of a defect can be now defined as

$$E_k = \frac{A_k}{R_k}. \quad (3)$$

The likelihood of a defect is high when the total area A_k of blobs in cluster is high (big blobs), and when they are concentrated within small radius R_k. This is demonstrated on the left cluster in Fig.7, where E amounts to 1.12. On the right cluster, with dust on the surface, this parameter amounts to only 0.27. Testing on many other images revealed that this approach reliably separates actual defects, e.g. scratches and coagulated paint, from dust and other small irregularities that are spread over larger surfaces.

An important issue with the k-means algorithm is that it requires the user to specify the number of clusters k to be generated. A simple and popular solution is to inspect the dendrogram produced using hierarchical clustering to see if it suggests a particular number of clusters. For example, the Elbow method looks at the total TSS as a function of the number of clusters and proposes to choose the number of clusters so that adding another cluster does not improve the total TSS considerably. In our test we did not observe TSS but the maximum E_k as the function of the number of clusters k. Table 1. shows the results of such an analysis for a single image.

Table 1. The parameter E with respect to the number of clusters k.

k	max(E_k)
2	0.338
3	0.579
4	0.753
5	0.757
6	0.850
7	0.853

The cluster with the maximum E_k was always in the same location when k > 2. If k is 4 and 5, E_k is almost the same, indicating that the elbow is around 4. By repeating this test on other images, similar results are achieved. For this reason, we use k = 4 at k-means clustering.

5. Conclusion

The difference image acquisition and processing method reliably reveals surface defects on black shiny KTL-coated parts. For its successful operation, a reference image of the background is required. It must be aligned with the examined image and acquired within same lightening conditions. This could be a problem without controlled environment. An automated inspection device is therefore carefully designed to meet all these requirements. In many cases surface defects are visible as concentrated groups of small blobs. For that purpose, a special parameter E, which defines the likelihood of a defect in a cluster, is developed. Serial production testing has shown that apart from the parameter E, the maximum blob size should still be considered for selecting defective parts. The presented inspection device eliminates defective parts from further processes. Furthermore, we are interested in providing feedback on the KTL coating process, by providing the type, location and frequency of defects. The most demanding task here is to identify the type of defect, because various defects look similar in the image. We did several initial tests with neural networks, but very ambiguous results were achieved because of similarities. Our future work is therefore aimed at the improvement of the measuring systems, as well at the identification of additional parameters that will contribute to a clearer definition of the defect type.

Acknowledgements

This work was supported by the Ministry of Higher Education, Science and Technology of the Republic of Slovenia, research program P2-0270, and by the TPV Group. The authors would also like to thank the staff of the TPV for their assistance and support in this research work.

References

[1] "E-Coat (KTL)." [Online]. Available: http://www.elameta.lt/e-coat-ktl.html. [Accessed: 10-Feb-2019].

[2] S. Satorres Martínez, C. Ortega Vázquez, J. Gámez García, and J. Gómez Ortega, "Quality inspection of machined metal parts using an image fusion technique," *Measurement*, vol. 111, pp. 374–383, 2017.

[3] L. Arnal, J. E. Solanes, J. Molina, and J. Tornero, "Detecting dings and dents on specular car body surfaces based on optical flow," *J. Manuf. Syst.*, vol. 45, pp. 306–321, 2017.

[4] A. Isasi-Andrieu, E. Garrote-Contreras, P. Iriondo-Bengoa, D. Aldama-Gant, and A. Galdran, "Deflectometry setup definition for automatic chrome surface inspection," in *IEEE International Conference on Emerging Technologies and Factory Automation, ETFA*, 2018.

[5] F. Pernkopf and P. O'Leary, "Image acquisition techniques for automatic visual inspection of metallic surfaces," *NDT and E International*. 2003.

[6] C. Jian, J. Gao, and Y. Ao, "Automatic surface defect detection for mobile phone screen glass based on machine vision," *Appl. Soft Comput.*, vol. 52, pp. 348–358, 2017.

[7] C. Fernandez, C. Platero, P. Campoy, and R. Aracil, "Vision system for on-line surface inspection in aluminum casting process," in *Proceedings of IECON '93 - 19th Annual Conference of IEEE Industrial Electronics*, 1993, pp. 1854–1859 vol.3.

[8] "TPV Group." [Online]. Available: https://www.tpv.si/en/. [Accessed: 10-Feb-2019].